FERRET

A FLEXIBLE NATURAL GAS MEMBRANE REFORMER FOR M-CHP APPLICATIONS

FCH JU GRANT AGREEMENT NUMBER: 621181

Start date of project: 01/04/2014 **Duration: 3 years**

WP4 – Lab-scale reformer development

D 4.1
First theoretical comparison between novel reactor configurations

Application area: SP1-JTI-FCH.3: Stationary Power Generation & CHP
Topic: SP1-JTI-FCH.2013.3.3 Stationary Power and CHP Fuel Cell System Improvement Using Improved Balance of Plant Components/Sub-Systems and/or Advanced Control and Diagnostics Systems
Funding scheme: Collaborative Project
Call identifier: FCH-JU-2013-1

Due date of deliverable: 31-05-2015	Actual submission date: 26-05-2014	Reference period: 01-04-2014 – 26-05-2015
Document classification code (*): FERRET-WP04-D42-DLR-TUE-26052015-v01.doc		Prepared by (**): TUE

Version	DATE	Changes	CHECKED	APPROVED
v0.1	26-05-2015	First Release	TUE-VS	TUE-FG

Project co-funded by the FCH JU within the Seventh Framework Programme (2007-2013)		
Dissemination Level		
PU	Public	X
PP	Restricted to other programme participants (including the Commission Services)	
RE	Restricted to a group specified by the consortium (including the Commission Services)	
CO	Confidential, only for members of the consortium (including the Commission Services)	
CON	Confidential, only for members of the Consortium	

(*) for generating such code please refer to the Quality Management Plan, also to be included in the header of the following pages

(**) indicate the acronym of the partner that prepared the document

Content

1. EXECUTIVE SUMMARY

1.1. Description of the deliverable content and purpose

The main tasks of this WP are the integration of catalyst and membranes and the testing of the reactor at lab scale and the model of the system. In particular this deliverable focuses on the first theoretical comparison of the different reactor configurations possible for the autothermal reforming of methane with membrane reactors. These configurations include packed beds and fluidized bed membrane reactors operated with vacuum or with sweep gas in the permeate side in order to increase the driving force for the hydrogen permeation.

The deliverable reports the models used for the simulations and the main results in terms of hydrogen permeation rates, concentration profiles and conversion rates.

1.2. Brief description of the state of the art and the innovation brought

1.3.- Deviation from objectives

N/A

1.4. If relevant: corrective actions

N/A

1.5. If relevant: Intellectual property rights

N/A

2. Introduction

In this report different membrane reactor configurations for auto-thermal reforming of methane are compared. The reactor model used for the comparison is simplified as follows: methane is fed in the system with H_2O and air at the feed side. Due to the presence of a Ni-based catalyst the Methane is converted into H_2-rich syngas and simultaneously, the H_2 is permeated through the membrane as in Figure 1.

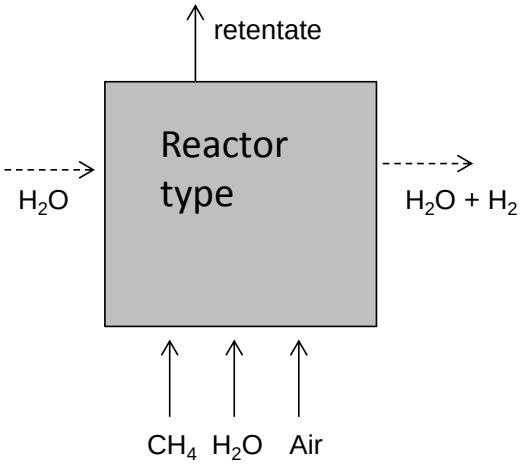

Figure 1: generic membrane reactor

H_2 permeates through the membrane with high purity (perm-selectivity of H_2 against the other components is supposed to be infinite). The driving force of the permeation is the difference of H_2 partial pressure between the feed and the permeate side.

The comparison has been carried out using both packed bed (PBR) and fluidized bed (FBR) configurations. In this report the following plants will be compared:

Membrane assisted packed bed reactor using vacuum conditions (0.03 bar) at the permeate side without sweep gas and adiabatic conditions in order to take into account the effect of the temperature profile (referred as MA-PBR/adiabatic in Figure 2a)

Membrane assisted packed bed reactor using steam (1 bar) as sweep gas at the permeate side fed to the system co-currently respect to the fuel gasses (referred as MA-PBR/co-current in Figure 2b) and counter-currently (referred as MA-PBR/counter in Figure 2c).

Fluidized bed reactor using vacuum condition at the permeate side (0.03 bar) which is defined as FBR/vacuum (Figure 3).

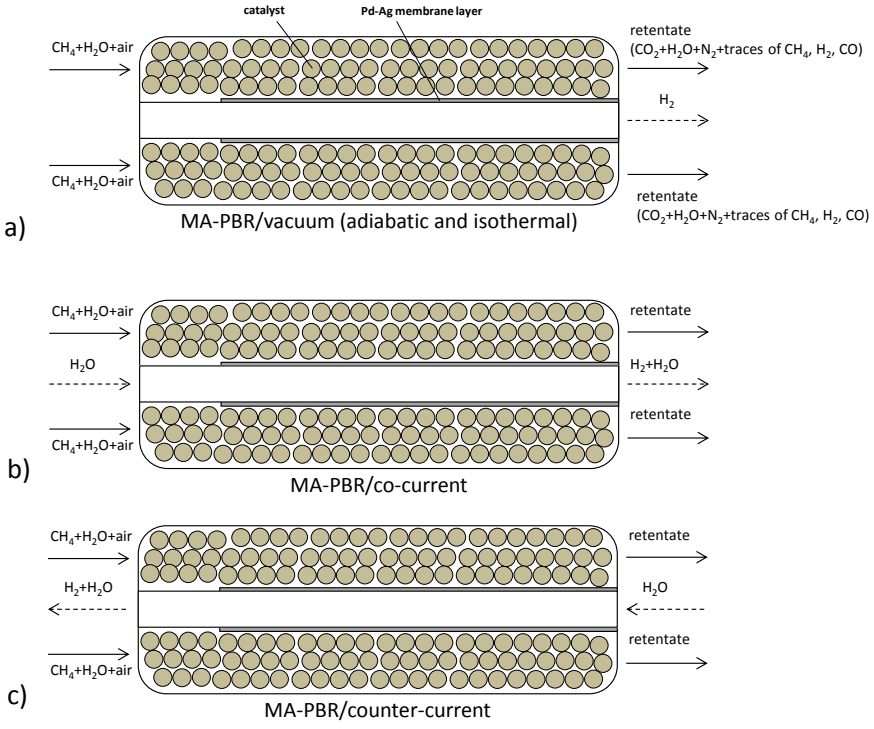

Figure 2: Membrane Assisted Packed Bed Reactor configurations

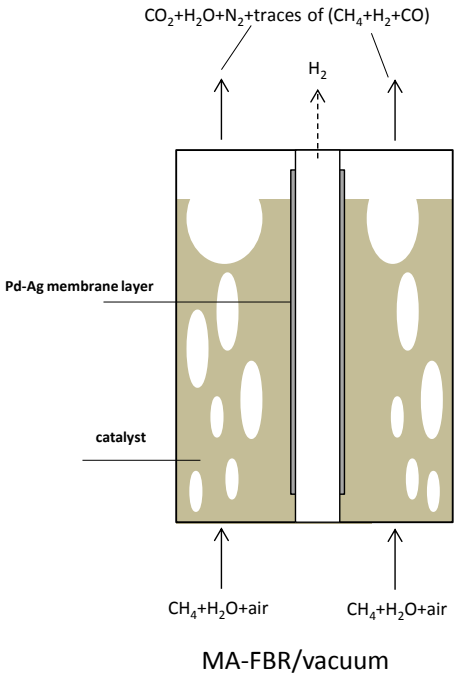

Figure 3: Membrane Assisted Fluidized Bed Reactor configuration

The analyses are based on a dedicated kinetic model and permeation model for auto-thermal reforming reactions and Pd-based membranes, respectively.
All the comparison has been carried out using CH_4 (80 mol/h), with a steam-to-carbon ratio equal to 3 (240 mol/h) and oxygen-to-carbon ratio equal to 0.755 (air flow rate equal to 143.8 mol/h with O_2 and N_2 mol equal to 21% and 79%, respectively)
The feed temperature has been selected equal to 600 °C and the operating pressure at feed side is equal to 10 bar.

Description of the models
The analysis of the system is carried out assuming the system under steady-state conditions and therefore no dynamic operations have been considered (no start-up has been modelled). The analysis is based on a pseudo-homogeneous one-dimensional model in which: i) no radial effect in the temperature profile; ii) the gas are perfectly mixed and there is no mass transfer limitation occurring from the bulk phase to the membrane surface (concentration polarization are neglected); iii) no diffusion limitations are occurring inside the catalyst.

Kinetic model
The kinetic model used for the analysis has been taken from Numaguchi and Kikuchi [1]. The reaction mechanism is based on the following three reactions:
SMR: $CH_4 + H_2O \leftrightarrow 3H_2 + CO$
MC: $CH_4 + 2O_2 \rightarrow 2H_2O + CO_2$
WGS: $CO + H_2O \leftrightarrow H_2 + CO_2$

The reaction rates R [mol $m^{-3}s^{-1}$] of the abovementioned reactions are calculated as follows (Table 1):

Table 1: kinetic model expressions

Reaction rates expressions

$$R_{MC} = \frac{k_{a.MC}\, p_{CH4}\, p_{O2}}{\left(1 + K^{ox}_{CH4} p_{CH4} + K^{ox}_{O2} p_{O2}\right)^2} + \frac{k_{b.MC}\, p_{CH4}\, p_{O2}}{\left(1 + K^{ox}_{CH4} p_{CH4} + K^{ox}_{O2} p_{O2}\right)}$$

$$R_{SMR} = \frac{k_{SMR}\left(p_{CH4}\, p_{H2O} - p^3_{H2}\, p_{CO} / K_{eq,SMR}\right)}{p^{1.596}_{H2O}}$$

$$R_{WGS} = \frac{k_{WGS}\left(p_{CO}\, p_{H2O} - p_{H2}\, p_{CO2} / K_{eq,WGS}\right)}{p_{H2O}}$$

	Pre exponential factor	Activation energy (kJ/mol)
$k_{a,MC}\,(mol\ s^{-1} m^{-3}_{react}\ \mathrm{bar}^{-2})$	$5.51 \cdot 10^{8}$	86.0
$k_{b,MC}\,(mol\ s^{-1} m^{-3}_{react}\ \mathrm{bar}^{-2})$	$4.64 \cdot 10^{8}$	86.0
$k_{SMR}\,(mol\ s^{-1} m^{-3}_{react}\ \mathrm{bar}^{-0.404})$	$1.78 \cdot 10^{8}$	106.9
$k_{WGS}\,(mol\ s^{-1} m^{-3}_{react}\ \mathrm{bar}^{-1})$	$1.67 \cdot 10^{5}$	54.5
$K^{ox}_{CH4}\,(bar^{-1})$	$1.26 \cdot 10^{-1}$	-27.3
$K^{ox}_{O2}\,(bar^{-1})$	$7.87 \cdot 10^{-7}$	-92.8
$\ln\left(K_{eq,SMR}\right) = \frac{-20009}{T(K)} - 22.82$		
$\ln\left(K_{eq,WGS}\right) = \frac{4400}{T(K)} - 4.036$		

The H_2 permeation has been calculated using the Sieverts' law the membrane permeability has been calculated according to experimental data.

The H_2 flux (ϕ''_{H2}) through the membrane is calculated as:

$$\phi''_{H2}(mol\ m^{-2} s^{-1}) = \frac{P_m}{t}\left(p^{0.5}_{H2,ret} - p^{0.5}_{H2,perm}\right)$$

where P_m *is equal to* $P_0 \times \exp\left(\frac{-E_a}{RT(K)}\right)$ with P_0 is equal to $6.135 \times 10^{-8} (mol\ m^{-1} s^{-1} Pa^{-0.5})$, E_a is equal to 7800 J/mol and t equal to $4.8 \times 10^{-6} \mu m$.

Reactor model

The packed bed reactor has been modelled as plug flow reactor (PFR). Mass and energy balances are solved according to the following general equations:

Gas phase mass balance

$$\underbrace{\varepsilon_g \frac{\partial \rho_g \omega_i}{\partial t}}_{\text{variation}} = \underbrace{-\frac{\partial \rho_g u_g \omega_i}{\partial z}}_{\text{convection}} + \underbrace{\frac{\partial}{\partial z}\left(\rho_g D_{ax} \frac{\partial \omega_i}{\partial z}\right)}_{\text{diffusion}} + \underbrace{\underbrace{n_i a_s}_{\text{reaction}} + \underbrace{\phi''_{m,i} a_m}_{\text{separation}}}_{\text{source}}$$

(1)

Gas phase energy balance (2)

$$\underbrace{\varepsilon_g \rho_g C_{p,g} \frac{\partial T}{\partial t}}_{\text{variation}} = \underbrace{-C_{p,g} \rho_g u_g \frac{\partial T}{\partial z}}_{\text{convection}} + \underbrace{\frac{\partial}{\partial z}\left(\lambda_g \frac{\partial T}{\partial z}\right)}_{\text{diffusion}} + \underbrace{\underbrace{\sum_{i=1}^{n_c} n_i a_s H_i}_{\text{reaction}} + \underbrace{\sum_{i=1}^{n_c} \phi''_{m,i} a_m H_i}_{\text{separation}} + \underbrace{\alpha_{b\to w} a_w \left(T - T_w\right)}_{\text{losses}}}_{\text{source}}$$

In which the accumulation term is zero (due to the steady-state condition), the diffusion term is neglected (based on the PFR assumptions) and the source term is obtained from the reaction occurring at the gas phase and the H_2 separation. In case of equation (2) the source term also includes the heat losses from the system which are however not considered at this stage (the reactor is in fact modelled as adiabatic).

The calculation of enthalpies of the single species are based on NASA polynomial coefficient for the calculation of the specific heat capacity (equations (3) a (4)).

Heat capacity

$$c_p \left[\frac{J}{molK}\right] = R \times \left(\frac{\alpha_5}{4} \times T^4 + \frac{\alpha_4}{3} \times T^3 + \frac{\alpha_3}{2} \times T^2 + \alpha_2 \times T + \alpha_1\right) \text{ (T in K)} \quad (3)$$

Enthalpy

$$H_i(T) \left[\frac{J}{mol}\right] = H_{298}^0 + \int_{298}^{T} c_{p.i}(T) dT \quad (4)$$

The membrane assisted fluidized bed model merged the concept of reaction kinetics with bed hydrodynamics and gas separation. A one dimensional two-phase fluidization model is considered for the simulation of fluidized bed membrane reactor. This model has been developed in the past years and used for different process involving H_2/O_2 membrane reactors [2,3]. There are two phase considered in the reactor i.e. bubble phase and emulsion phase. The schematic of the reactor model is a combination of different continuous stirred tank reactors (CSTRs) simulating the emulsion phase, while each section consists of further sub CSTRs simulating the bubble phase. In this way the emulsion phase can be simulated with a certain back mixing degree, while the bubble phase remains at fairly plug flow conditions. The H_2 permeates through the membrane from both the emulsion and the bubble phase, which however have different gas composition due to the bubble-to-emulsion phase mass transfer resistance which is accounted for in the model. For the MA-FBMR, the overall energy balance is solved while the fluidized bed temperature is assumed to be uniform along the bed.

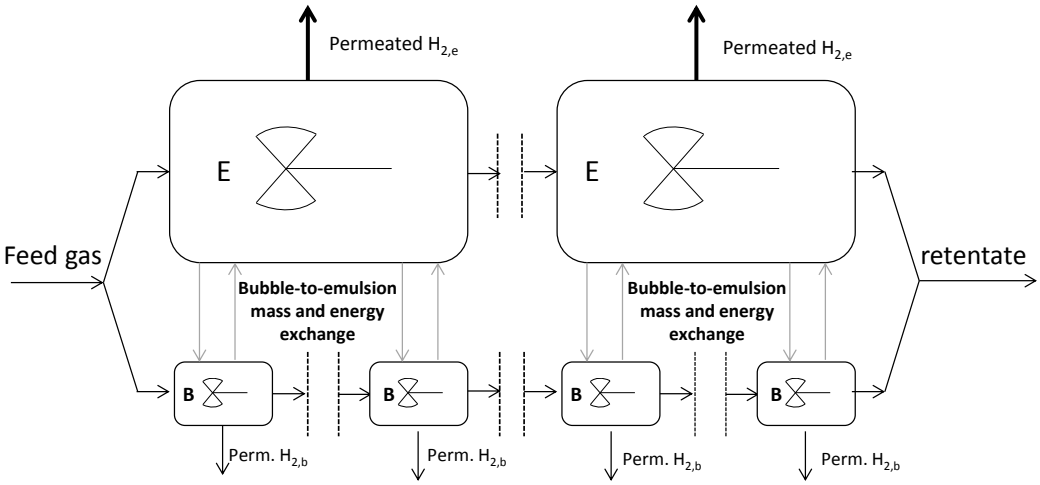

Figure 4: Schematic of the MA-FBR model

Moreover, the model also assumes that the gas passing through the emulsion phase is at minimum fluidization velocity and is properly mixed in each section while the remaining gas flows as bubbles. The gas permeated from both bubble and emulsion phase through membranes is distributed on the basis of local bubble fractions. Meanwhile, the gas separated from emulsion phase is immediately compensated through bubble phase (to keep the emulsion phase at minimum fluidization). The gas compensated through bubbles phase is depends on the value of bed voidage (bed expansion). The bed voidage (ε) represents the division of membrane area between bubble and emulsion phase. A constant temperature is considered across the reactor bed with no heat loses to the surroundings. The correlations and equation used in the modelling are shown in Table 2.

Table 2: Hydrodynamic parameters used in the modelling

Parameters	Equation	Ref.
Archimedes number	$Ar = {d_p}^3 \rho_g(\rho_p - \rho_g) g/{\mu_g}^2$	[4]
Minimum fluidization velocity	$U_{mf} = (\mu_g/d_p\rho_g)\left(\sqrt{(27.2)^2 + 0.0408Ar} - 27.2\right)$	[5]
Bed voidage at minimum fluidization velocity	$\varepsilon_{mf} = 0.586Ar^{-0.029}\left(\frac{\rho_g}{\rho_p}\right)^{0.021}$	[5]
Velocity of rise of swarm of bubbles	$U_b = U_o - U_{mf} + U_{br}$	[4]
Rising velocity of single bubble	$U_{br} = 0.711(g d_{b,avg})^{1/2}$	[4]
Emulsion velocity	$U_e = \frac{U_o - \delta U_b}{1 - \delta}$	[4]
Average bubble diameter	$d_{b,avg} = d_{b,max} - (d_{b,max} - d_{bo})\exp\left(-\frac{0.3H}{D_T}\right)$	[6]
Initial bubble diameter	$d_{bo} = 0.376(U_o - U_{mf})^2$	[3]
Bubble phase fraction	$\delta_{bn} = \frac{{U_b}^s}{U_b}$	[3]
Emulsion phase fraction	$\delta_{en} = 1 - \delta_{bn}$	[3]
Maximum superficial bubble gas velocity	${U^s}_{b,max} = U_o - U_{mf}$	[3]
Initial superficial bubble gas velocity	${U^s}_{b,o} = U_{br,o}\delta_{bo}$ where $\delta_{bo} = (1 - H_{mf}/H_f)$	[3]
Height of bed at minimum fluidization velocity	$H_{mf} = H_s\frac{1 - \varepsilon_s}{1 - \varepsilon_{mf}}$	[6]
Height of bed expansion	$H_f = H_{mf}\frac{C_1}{C_1 - C_2}$ where, $C_1 = 1 - \frac{U_{b,o}}{U_{b,avg}} exp\left(-\frac{0.275}{D_T}\right)$ $C_2 = \frac{{U_b}^s}{U_{b,avg}}\left[1 - exp\left(-\frac{0.275}{D_T}\right)\right]$	[3]

Average bubble rise velocity	$U_{b,avg} = U_o - U_{mf} + 0.711(g d_{b,avg})^{1/2}$	[3]
Gas exchange coefficient	$K_{bc} = 4.5\left(\frac{U_{mf}}{d_p}\right) + 5.85\left(\frac{D_g^{1/2} g^{1/4}}{d_b^{5/4}}\right)$ $K_{ce} = 6.77\left(\frac{D_g \varepsilon_{mf} U_b}{d_b^3}\right)^{1/2}$ $\frac{1}{K_{be}} = \frac{1}{K_{bc}} + \frac{1}{K_{ce}}$	[3]

Analysis of the results

The reactor design for the considered configurations has been carried out in order to reach about 5 Nm^3/h of pure H_2 at the permeate side. The geometry of the reactor is shown in Figure 5. Four membranes of 1 cm diameter are used in the system. For each system the reactor length (and therefore the membrane length) is calculated in order to get the required H_2.

Packed bed configurations

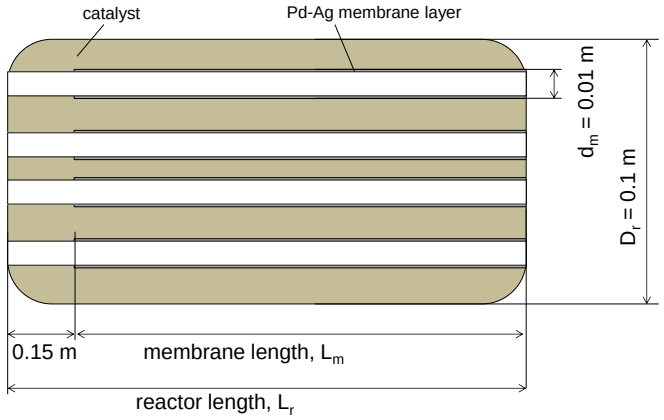

Figure 5: MA-PBR geometry

For MA-PBRs the results are shown in Table 1. For the counter-current configuration three different scenarios have been considered at the permeate side: i) high sweep gas and low pressure (500 mol h^{-1} and 1 bar), ii) low sweep gas and low pressure (100 mol h^{-1} and 1 bar); high sweep gas and high pressure (500 mol h^{-1} and 3 bar).
Depending on the gas flow rate, the hydrogen recovery factor HRF[1] is in the range of 85.5-86.5%.

Table 3: overall results for MA-PBR system

	MA-PBR					
	iso-thermal	adiabatic	co-current		counter	
sweep gas, mol h^{-1}	0	0	500	500	100	500
p_{H2}, bar	0.03	0.03	1	1	1	3
H_2 flow, mol h^{-1}	223.20	224.56	222.93	223.92	222.81	222.48
H_2 flow, Nm^3 h^{-1}	5.00	5.03	5.00	5.02	4.99	4.99
HRF	86.0%	86.5%	85.9%	86.3%	85.8%	85.7%
reactor length, m	0.50	0.45	0.63	0.57	0.75	0.76
Membrane Area,	0.062	0.057	0.079	0.072	0.094	0.096

[1] $HRF = \frac{H_{2,p}}{4 \times CH_{4,feed} - 2 \times O_{2,air}}$

m^2						
H_2, flux, mol h^{-1} m^{-2}	3588.15	3971.13	2838.41	3126.12	2380.00	2329.57

For the MA-PBR cases, the composition at the retentate side is shown in Table 4. The results are the practically the same for the all cases and the differences are mostly related to the different HRF.

Table 4: Retentate composition

Retentate composition	iso-thermal	adiabatic	MA-PBR co-current	counter		
sweep gas, mol h^{-1}	0	0	500	500	100	500
p_{H2}, bar	0.03	0.03	1	1	1	3
H_2	6.5%	6.5%	7.2%	6.3%	6.7%	6.7%
H_2O	40.7%	40.6%	40.2%	40.8%	40.6%	40.7%
CO	1.5%	1.4%	1.4%	1.5%	1.5%	1.5%
CO_2	19.9%	20.0%	20.0%	19.9%	19.8%	19.8%
CH_4	0.5%	0.4%	0.3%	0.5%	0.5%	0.5%
O_2	-	-	-	-	-	-
N_2	31.0%	31.0%	30.8%	31.0%	30.9%	30.9%

The systems operated under vacuum conditions show the highest H_2 flux due to the high driving force associated and therefore the membrane area is lowest compared to the other cases. Compared to iso-thermal case, the adiabatic configuration shows slightly better results mostly because the reactor has an average temperature (along the profile) higher than 600°C and only at the reactor outlet it is 600°C as it can be seen from Figure 7. It is possible to notice that the combustion reaction (MC) occurs at the reactor inlet and therefore all the oxygen is immediately consumed. After that, the SMR and WGS reactions start and the H_2 is produced up to almost 0.25 of mol fraction. When the H_2 permeation starts (at the reactor length equal to 0.15 m) the H_2 fraction start to decreases, the CH_4 is consumed faster and the CO_2 increases.

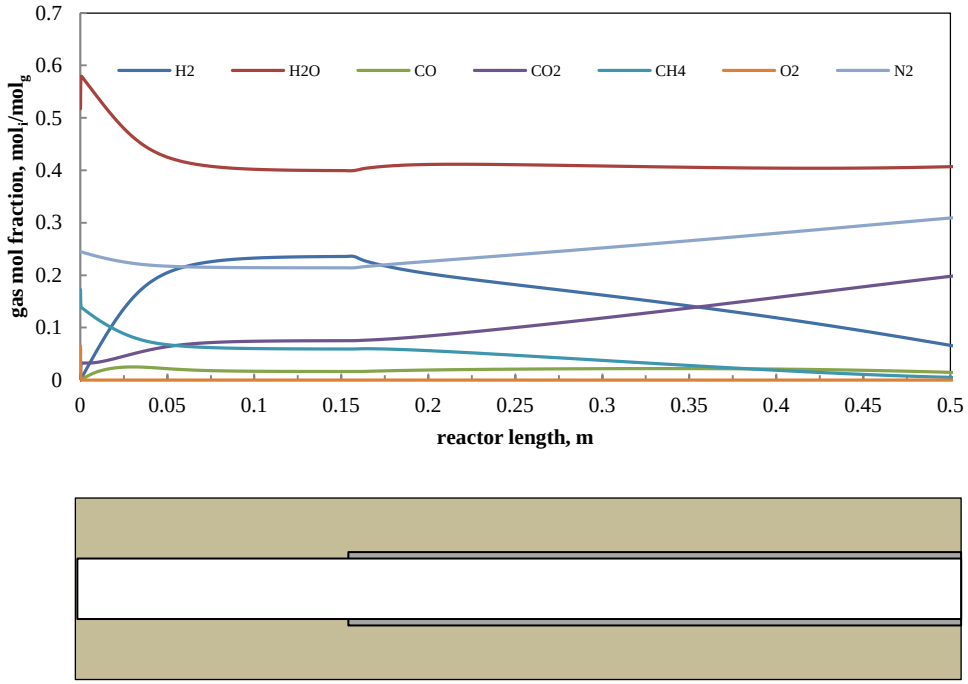

Figure 6: Composition profile along the reactor at the retentate side.

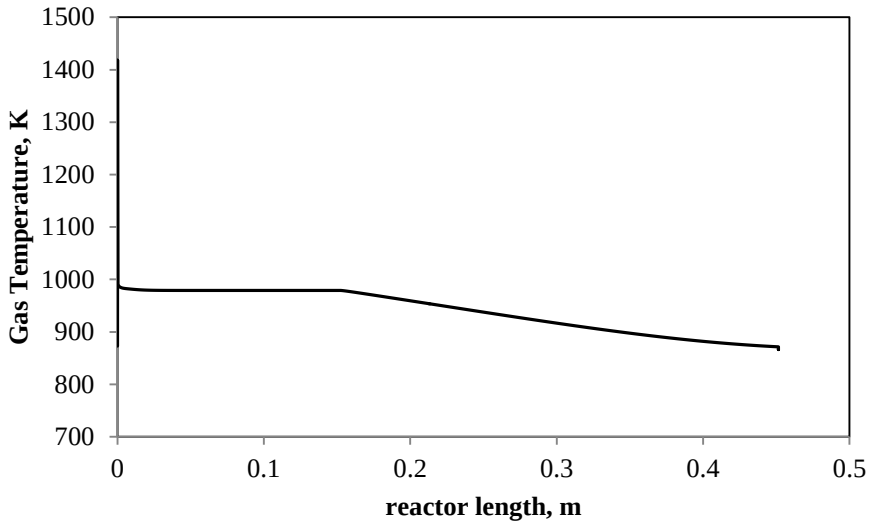

Figure 7: Gas temperature profile along the reactor for the adiabatic case.

In case of sweep gas, the H_2 is separated at higher pressure (1 bar vs 0.03 bar) which results beneficial for the balance of the entire system. However, in case of co-current feeding the membrane area required is higher than in case of counter-current feeding (with the same pressure and sweep gas). This can be explained by looking at the H_2 partial pressure profile in Figure 8. The sensitivity analysis of the counter-current cases is shown in Figure 9 and it is possible to notice the different partial pressure profile at the permeate side.

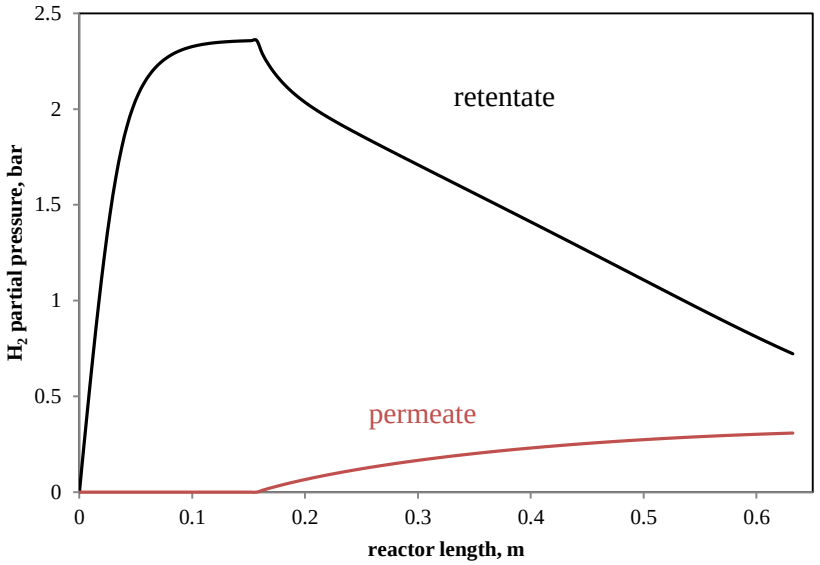

a)

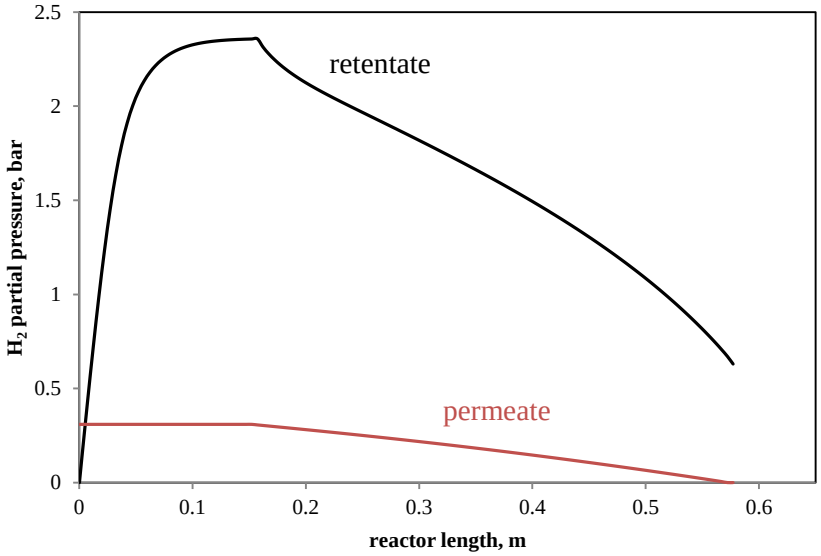

b)

Figure 8: H_2 partial pressure profiles at the retentate and permeate sides and H_2 flow rate passing through the membrane (dashed line) for MA-PBR/co-counter (a) and MA-PBR/counter (500-1 bar)

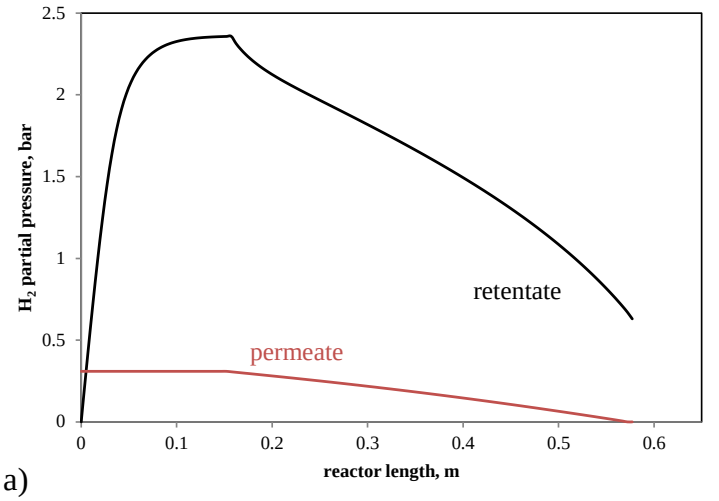

a)

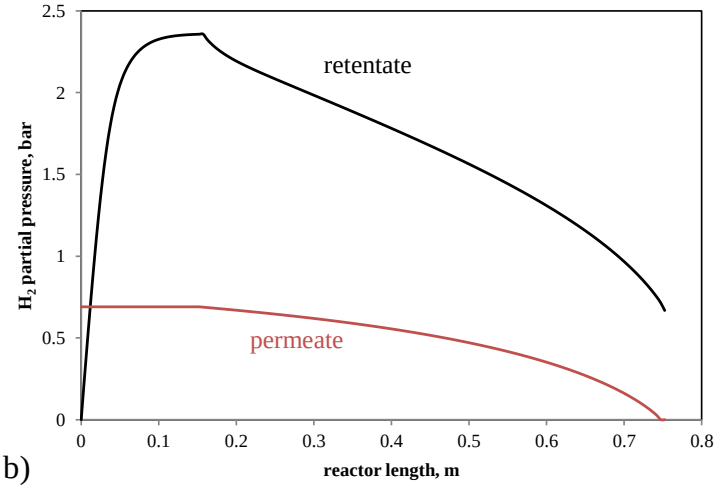

b)

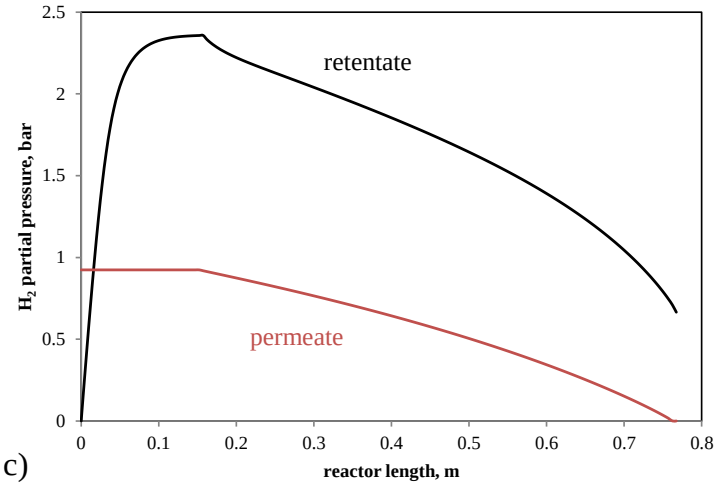

c)

Figure 9: H_2 partial pressure profiles at the retentate and permeate sides and H_2 flow rate passing through the membrane (dashed line) for MA-PBR/counter configuration:(a) low pressure-high sweep gas (500 mol $^{h-1}$ 1 bar);(b) low pressure low-low sweep gas (100 mol h^{-1}, 1 bar) and (c) high pressure-low sweep gas (500 mol h^{-1} 3 bar)

Fluidized bed configuration

As discussed in the previous paragraph, the fluidized bed reactor is simulated as a combination of CSTR in order to take into account the effect of gas back-mixing which is typical of a fluidized bed reactors. The

gas back-mixing depends on several parameters which are not taken into account at this stage. Since an experimental comparison would be required in order to quantify the real effect on the gas profile, three different configurations have been considered for the system. The effect of the number of CSTR used for the discretization of the entire reactor is significantly important in the emulsion phase, because in the bubble phase the gas-back mixing is almost negligible. In order to have an overview of the possible results four different cases have been considered in this analysis: i) in the first case only 1 CSTR is used for the emulsion phase (high back-mixing here referred as H-BM); ii) in the second case 3 CSTRs are considered for the emulsion (high-intermediate back-mixing here referred as HI-BM); iii) in the third case 5 CSTRs are considered for the emulsion (low-intermediate back-mixing here referred as LI-BM); iv) finally 10 CSTRs are considered for the emulsion (almost no effect of back mixing as for the plug flow reactor here referred as PF-BM). For the bubble phase 5 CSTRs (per single CSTR used in the emulsion phase) are always assumed.
As for the MA-PBR configurations, in this case the comparison have been carried out using a fixed gas flow rate, O/C and S/C (the same condition are used), a fixed reactor diameter D_r equal to 0.15 m (in the previous case the D_r was selected 0.1 m) in order to be always in a bubbling fluidization regime ($3<u_0/u_{mf}<5$) where most of the equation listed in Table 2 are valid, and the reactor and membrane length are varied in order to reach the desired HRF for 5 Nm^3/h of H_2.
The results of the analysis are reported in Table 5: it is possible to notice that at increased number of CSTR in the emulsion phase the H_2 flux increases and the reactor becomes smaller (and therefore also the membrane area decreases). This is because at higher gas back-mixing there is an increased dilution of the H_2 and therefore more membrane is required for the separation. Compared to the MA-PBR/adiabatic the membrane area is oscillating between -20% and +10% depending on the number of CSTR considered.

Table 5: overall results for MA-FBR system

	H-BM	HI-BM	LI-BM	PF-BM
N_R of CSTR at the emulsion phase	1	3	5	10
H_2 flow, mol h^{-1}	222.89	223.23	223.03	223.28
H_2 flow, Nm^3 h^{-1}	5.00	5.00	5.00	5.00
HRF	85.9%	86.1%	86.0%	86.1%
reactor length, m	0.52	0.40	0.38	0.37
Membrane Area, m^2	0.065	0.05	0.048	0.046
H_2, flux, mol h^{-1} m^{-2}	3410.89	4497.27	4695.20	4815.28

The retentate gas composition is shown in Table 6 for the different cases. As expected, due to the very similar HRF, the predicted composition is practically the same for the all systems.

Table 6: Retentate composition for the studied cases.

Retentate composition	H-BM	HI-BM	LI-BM	PF-BM

H_2	7.1%	6.8%	6.7%	6.5%
H_2O	40.0%	40.2%	40.3%	40.4%
CO	1.7%	1.6%	1.6%	1.6%
CO_2	19.7%	19.8%	19.7%	19.7%
CH_4				
O_2	-	-	-	-
N_2	31.2%	31.3%	31.3%	31.3%

Finally for the LI-BM system the gas profile is also shown in the Figure 10 for both emulsion and bubble phases. It can be noticed that the main difference between emulsion and bubble phase is the gas conversion, which is lower for the bubble phase. It can be explained by looking at the kinetic model in which the reaction rate is dependent on the mass of the catalyst: in the bubble phase the solid is only present in the wake and, for a negligible amount also inside the bubble while in the emulsion phase the amount of solid is significantly higher. However due to the mass transfer between the bubble and the emulsion phase the final composition of the gas in the two phases is very close.

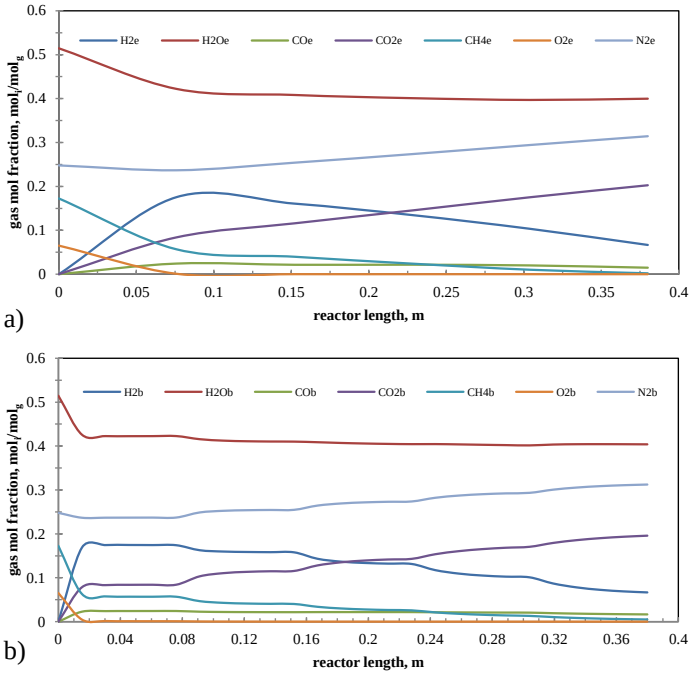

Figure 10: retentate gas composition profile for the MA-FBR/LI-MB in the emulsion (a) and bubble (b) phase.

Conclusions

The preliminary analysis of membrane reactor for auto-thermal reforming of methane to produce 5 Nm^3/h of H_2 has been carried in this deliverable. Two different reactor concepts have been compared: in the first case the membranes are located in a packed bed reactor which works with different conditions at the permeate side; in the second case, a fluidized bed reactor is used which is operated in bubbling regime. The results show that: i) for packed bed configuration, when the permeate side is at vacuum conditions, the H_2 flux is the highest, however this configuration is not interesting at industrial scale; ii) when using H_2O as sweep gas, the highest H_2 flux is achieved in counter-current feeding however the optimal conditions in terms of permeate pressure and/or sweep gas flowrate results from a techno-economic optimization; iii) in case of fluidized bed configuration, the H_2 flux is higher than in the case

with packed bed reactor although the reactor requires a bigger diameter (50% bigger) to achieve the desired fluidization regime; iv) however a more refined model should be considered in order to validate the strategy adopted for the modelling (i.e. selection of the number of CSTRs for the different phases for fluidized bed and concentration polarization for the packed bed model) and the mass transfer model adopted in this study.

References

[1] T. Numaguchi, K. Kikuchi, Intrinsic kinetics and design simulation in a complex reaction network; steam-methane reforming, Chem. Eng. Sci. 43 (1988) 2295–2301.

[2] F. Gallucci, M. Annaland, J. Kuipers, Autothermal reforming of methane with integrated CO_2 capture in a novel fluidized bed membrane reactor. Part 1: experimental demonstration, Top. Catal. 51 (2008) 133–145.

[3] F. Gallucci, M. Annaland, J. Kuipers, Autothermal reforming of methane with integrated CO_2 capture in a novel fluidized bed membrane reactor. Part 2 comparison of reactor configurations, Top. Catal. 51 (2008) 146–157.

[4] D. Kunii, O. Levenspiel, Fluidization Engineering, Elsevier, 1991.

[5] C.-Y. Shiau, C.-J. Lin, Equation for the superficial bubble-phase gas velocity in fluidized beds, AIChE J. 37 (1991) 953–954.

[6] S. Mori, C.Y. Wen, Estimation of bubble diameter in gaseous fluidized beds, AIChE J. 21 (1975) 109–115.